



# An experimental study to swing up and control a pendulum with two reaction wheels

João F. S. Trentin · Samuel da Silva · Jean M. de S. Ribeiro · Hanspeter Schaub

Received: 7 May 2020 / Accepted: 20 January 2021 / Published online: 3 February 2021  
© Springer Nature B.V. 2021

**Abstract** An experimental study is discussed on a strategy that combines on-off and sliding mode control to swing up and control a pendulum with two reaction wheels in the upright position. The control scheme uses only one reaction wheel at a time, adapting the control law to turn off one of the control actions. The design takes into account the plant limitations, thus justifying the combination of the two strategies. The mechanical differences between the standard reaction wheel pendulum configuration and the one studied in this paper are pointed out to explain the use and the operation of the controller. Additionally, two cases are studied to verify

experimentally the performance of the controller designed using low-cost hardware for real-time tests.

**Keywords** Reaction wheels · Nonlinear dynamics · Pendulum · Sliding mode control · Swing-up

## 1 Introduction

The control and stabilization of inverted pendulums have been studied for decades. Although these systems seem to be straightforward, they have many attractive characteristics, such as nonminimum phase, instability, nonlinearities, and under-actuation, that motivate research. They are often used as benchmarks to test new controllers as well as new arrangements of actuators. A few examples of these systems are: the reaction wheel pendulum [14], the wheeled inverted pendulum [4], the pendulum on a cart system [9], the reaction mass pendulum [10], the reaction wheel unicycle [8], the pendulum with two reaction wheels [16], among others. Due to the particularities of each of the systems, the tested controllers present many different features, including swing-up strategies which were mainly tested on the pendulum on a cart system and in the reaction wheel pendulum. For instance, considering the pendulum on a cart, some interesting techniques are presented in [2, 9].

---

J. F. S. Trentin (✉) · S. da Silva  
Department of Mechanical Engineering, São Paulo State University (UNESP), Avenida Brasil 56,  
Ilha Solteira 15385-000, SP, Brazil  
e-mail: joao.trentin@unesp.br

S. da Silva  
e-mail: samuel.silva13@unesp.br

J. M. d. S. Ribeiro  
Department of Electrical Engineering, São Paulo State University (UNESP), Avenida Brasil 56,  
Ilha Solteira 15385-000, SP, Brazil  
e-mail: jean.ribeiro@unesp.br

H. Schaub  
Department of Aerospace Engineering Sciences,  
University of Colorado, Boulder, CO 80303-0429, USA  
e-mail: hanspeter.schaub@colorado.edu

There are some classical approaches to swing up a pendulum with a reaction wheel, e.g., Spong et al. [14] discuss a partial feedback linearization and passivity of the resulting zero dynamics to take the pendulum from the downward position to the region in which another control technique actuates to balance the pendulum in the upright position. Another approach to swing up the reaction wheel pendulum includes a combination of a sliding mode controller with a generalized PI [6]. In this case, the swing-up process is based on the desired trajectory tracking, where the amplitude of the pendulum oscillation is increased to drive the pendulum until the upright position. The choice of the desired trajectory using the system's energy is crucial to aid in the process of driving the pendulum to the upright position [6].

Srinivas and Behera [15] present two different swing-up control strategies that can be combined with any balancing scheme to stabilize the pendulum in the upright position. The first one is a sinusoidal swing-up scheme in which the amplitude of the signal is increased until the pendulum is close enough to the upright position to be able to switch to the balancing strategy. The second control strategy to swing up the reaction wheel pendulum concerns the real-time application of interconnection and damping assignment-passivity based control considering a constrained input case. Later, Jepsen et al. [7] present a switching strategy in which a bang-bang controller is combined with three criteria based on the system's energy. This bang-bang controller has to drive the pendulum until it reaches the region of the catch angle of the stabilizing controller. Thus, it needs to use two different controllers to swing up and stabilize the reaction wheel pendulum in the upright position.

More recently, Sowman et al. [13] demonstrate that nonlinear model predictive control could be an alternative to swing up and balance the reaction wheel pendulum in the upright position using a single controller. The performance of such a controller was also verified experimentally. Gutiérrez-Oribio et al. [5] propose the control and stabilization of the classical reaction wheel pendulum using a third-order discontinuous integral sliding mode algorithm. Although the analysis carried out has ensured only local finite-time convergence of the states to the origin, in the experiment, it was possible to drive the pendulum to the upright position using the proposed

approach releasing the pendulum from the downward position.

This brief literature review about the swing-up control strategies for pendulums actuated by reaction wheels focuses on the designs that are verified experimentally. Many other strategies are not addressed either because the experimental tests are not conducted, or they have discussed only on the balancing control strategies, where the pendulum is released around the unstable equilibrium point. However, these strategies have contributed significantly to the development of the control theory.

Nonetheless, this paper presents a swing-up approach based on the variable structure control (VSC) in which sliding mode constitutes a significant feature. It has attractive properties such as insensitivity to bounded uncertainties, disturbances, as well as parasitic dynamics [3, 12]. The designer chooses a custom function and designs a high-speed switching control law, usually divided into two parts: a switching part which is responsible for driving the system to the function and an equivalent one, which controls the system in the vicinity of the sliding function. The main objective of the control law is to drive the system to a sliding manifold, and once the sliding variable is zero and remains at zero, the control law will slide to the equilibrium point.

The pendulum configuration studied in this paper is based on the classical reaction wheel pendulum, but instead of having one reaction wheel, it has two. This different configuration is introduced in [16] which carry out a comparison of using one or two actuators controlled by a simple PID controller. Moreover, Trentin et al. [17] design nonlinear controllers for this new configuration, including a nonlinear proportional-derivative controller and a sliding mode controller. In this case, both reaction wheels are actuated and the sliding mode controller had a much better outcome. The performance of the nonlinear controllers are verified experimentally.

Thereby, the main contribution of this paper is to present an experimental study of a variable structure swing-up control law for a pendulum with two reaction wheels using only one of them at a time. One of the objectives is to evaluate if the controller designed can overcome many of the problems of the experimental device. The only measured variable in this study is the pendulum's angular position. Thus, there is no information regarding the reaction wheels'

rates. This makes the applicability of some control strategies impossible and unsuitable; once for many designs, there will not be enough information to guarantee the stability of the control laws that are proposed. Furthermore, the pendulum angular motion also presents a nonlinear behavior regarding the friction, where the equation of motion is updated to take into account dissipative effects by considering viscous and the Coulomb frictional models. This phenomenon is also considered in the controller design and it is identified in [17]. Since many of the parameters of the plant are inaccurate, the sliding mode control can be very useful and it is combined with the on-off control to deal with the limitations of the DC motors. Additionally, some particularities of this dynamic system with two reaction wheels are discussed to explain the adopted swing-up control strategy.

This paper is organized as follows: Sect. 2 covers the mathematical model of the pendulum with two reaction wheels, Sect. 3 shows how the swing-up control strategy based on sliding modes was conducted, Sect. 4 presents a brief experimental description of the plant and hardware used for tests and the experimental results obtained. It also explains the mechanical differences between the classical reaction wheel pendulum and the pendulum studied in this paper. Finally, Sect. 5 describes the concluding remarks of the paper.

## 2 Mathematical model

This section presents the mathematical model of the pendulum with two reactions that is shown in Fig. 1. The model of this pendulum configuration is first derived in [16] and complemented with a model for the friction torque in [17]. Here, we present directly the equation of motion of the pendulum with two reaction wheels and afterwards the motor torque equations. This model’s derivation was performed in the body (pendulum) fixed frame, not in the inertial one. Thus, the angular velocities and accelerations are evaluated in the body frame, which means that they are relative angular velocities and accelerations; they are not absolute ones.

The position control is performed through voltage inputs to the DC motors, that in turn, actuate the reaction wheels generating torques in order to provide

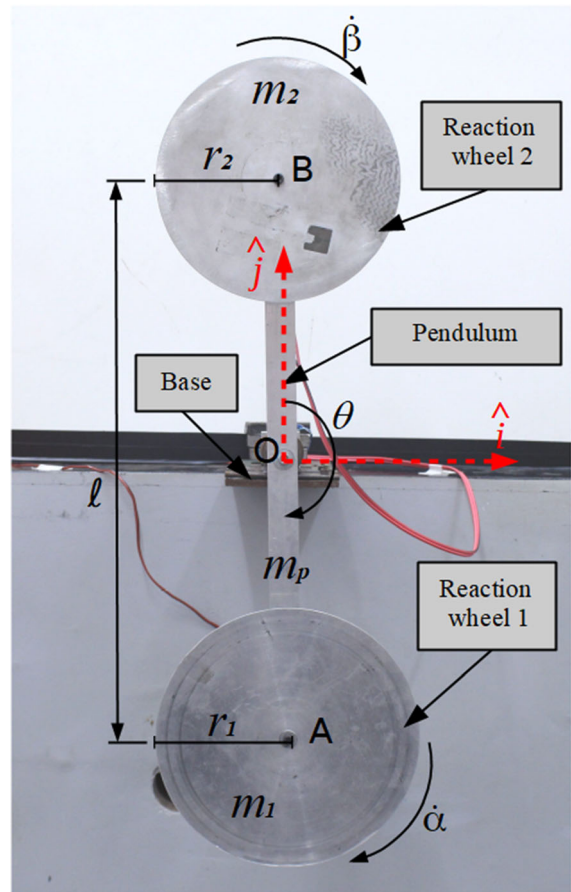


Fig. 1 Pendulum with two reaction wheels

an adequate output for the pendulum’s angular position. To do so, the system’s mathematical modeling is described. Therefore, the equation of motion of the pendulum with two reaction wheels is:

$$I_{zeq}^O \ddot{\theta} + I_{zw1}^A \ddot{\alpha} + I_{zw2}^B \ddot{\beta} = (m_1 - m_2)g \frac{\ell}{2} \sin \theta - T_{fr} \tag{1}$$

where  $\theta$  describes the pendulum angular motion and  $\ddot{\theta}$  its angular acceleration,  $\ddot{\alpha}$  is the angular acceleration of the reaction wheel 1 and  $\ddot{\beta}$  the angular acceleration of the reaction wheel 2.  $I_{zeq}^O$  is the moment of inertia of the pendulum and reaction wheels,  $I_{zw1}^A$  and  $I_{zw2}^B$  are the moments of inertia of reaction wheels 1 and 2, respectively, that are given by:

$$I_{zeq}^O = \frac{1}{2}(m_1 r_1^2 + m_2 r_2^2) + \frac{1}{4}(m_1 \ell^2 + m_2 \ell^2) + \frac{1}{12} m_p \ell^2 \tag{2}$$

$$I_{zw1}^A = \frac{1}{2} m_1 r_1^2 \tag{3}$$

$$I_{zw2}^B = \frac{1}{2} m_2 r_2^2 \tag{4}$$

The subscript 1 is related to the reaction wheel 1 and the subscript 2 to the reaction wheel 2 regarding the masses  $m$  and the radii  $r$ . Moreover,  $T_{fr}$  is the friction torque for which its model was updated to represent the friction of the experimental device:

$$T_{fr} = \text{sgn}(\dot{\theta}) (C_v |\dot{\theta}| + C_c) \tag{5}$$

where  $C_v = 0.0031$  Nms/rad is the coefficient of viscous friction, and  $C_c = 0.011$  Nm the Coulomb friction coefficient [17]. Additionally, the motor torques for each reaction wheel are:

$$T_1 = I_{zw1}^A \ddot{\theta} + I_{zw1}^A \ddot{\alpha} \tag{6}$$

$$T_2 = I_{zw2}^B \ddot{\theta} + I_{zw2}^B \ddot{\beta} \tag{7}$$

Coupling the DC motors model to the motor torque equations, and solving with respect to the variables of the voltages applied to them, yields:

$$V_\alpha = T_1 \frac{R_a}{K_t} + K_v \dot{\alpha} \tag{8}$$

$$V_\beta = T_2 \frac{R_a}{K_t} + K_v \dot{\beta} \tag{9}$$

where  $R_a = 1.06\Omega$  is the armature resistance,  $K_t = 0.0063$  Vs/rad is the motor torque constant, and  $K_v = 0.0063$  Nm/A is the back electromotive force constant. The other parameters based on the experimental device are  $m_1 = 0.21$  kg,  $r_1 = 0.11$  m,  $m_2 = 0.13$  kg,  $r_2 = 0.1$  m,  $m_p = 0.16$  kg and  $\ell = 0.5$  m. The mathematical model is described as input-output where the input is the voltage applied to the DC motors that depends on the motor torques, and the output is the pendulum’s angular position. Additional details can be seen in Fig. 3.

### 3 The controller design

There are many different swing-up control strategies already presented in the literature, as aforementioned. Here, the strategy is straightforward and combines an on-off controller with the sliding mode controller. The control law presented in this manuscript was first designed to use both reaction wheels at the same time, see [17]. However, we managed to adapt the control law to swing up the pendulum and control it in the upright position using just one of them at a time. This also took into account the limits of the DC motor; thus, the proposed sliding mode control law is combined with an on-off controller.

Firstly, the design of a sliding mode control using a sliding function is carried out as if both reaction wheels were used to control the pendulum. The use of this function is because the DC motors do not have encoders. Thereby, the angular velocities of the reaction wheels are unknown. Consequently, the sliding function takes into account the known states, which are the angular position and velocity of the pendulum. The tracking error is defined as  $e = \theta - \theta_d$ , where  $\theta_d$  is the desired pendulum angular position. The sliding function ( $\sigma(e, t)$ ) is given by:

$$\sigma(e, t) = \dot{e} + \gamma e \tag{10}$$

where  $\gamma$  is a positive constant, the system reaches the sliding function when  $\sigma(e, t) = 0$ , and if it remains at zero, it will slide to the equilibrium point. When analyzing the function presented in (10) in the error configuration space, it represents a straight line of sliding, and it must have its values tending to zero to assure the convergence in a finite time interval. The derivative of the sliding function yields:

$$\dot{\sigma} = \ddot{e} + \gamma \dot{e} \equiv \ddot{\theta} - \ddot{\theta}_d + \gamma \dot{e} \tag{11}$$

Selecting the following equation to be a candidate for the Lyapunov function, we have:

$$\mathcal{V}(\sigma) = \frac{1}{2} \sigma^2 \tag{12}$$

where this function must be positive definite with a negative definite derivative to be a Lyapunov function. Evaluating the derivative of (12), yields:

$$\dot{\mathcal{V}}(\sigma) = \sigma \dot{\sigma}, \sigma \neq 0 \tag{13}$$

Now, it is imperative to prove that the derivative of the candidate to be Lyapunov function is negative definite. Thus, rearranging the equation of motion presented in (1) and substituting it into the derivative of the sliding function in (11) leads to:

$$\begin{aligned} \dot{\sigma} = & \frac{(m_1 - m_2)g \frac{\ell}{2} \sin \theta}{I_{zeq}^O} - \begin{bmatrix} I_{zw1}^A & I_{zw2}^B \\ I_{zeq}^O & I_{zeq}^O \end{bmatrix} \begin{Bmatrix} \ddot{\alpha} \\ \ddot{\beta} \end{Bmatrix} + \\ & - \frac{T_{fr}}{I_{zeq}^O} - \ddot{\theta}_d + \gamma \dot{e} \end{aligned} \tag{14}$$

The  $2 \times 1$  desired states vector  $\boldsymbol{\eta} = \{\ddot{\alpha} \ddot{\beta}\}^T$  and the  $1 \times 2$  matrix  $[Q]$  are introduced to simplify the notation:

$$[Q] = \begin{bmatrix} I_{zw1}^A & I_{zw2}^B \\ I_{zeq}^O & I_{zeq}^O \end{bmatrix} \tag{15}$$

Furthermore, adopting the control law as:

$$\begin{aligned} [Q]\boldsymbol{\eta} = & \frac{(m_1 - m_2)g \frac{\ell}{2} \sin \theta}{I_{zeq}^O} - \frac{T_{fr}}{I_{zeq}^O} - \ddot{\theta}_d + \\ & + \gamma \dot{e} + \kappa \operatorname{sgn}(\sigma) \end{aligned} \tag{16}$$

Substituting the control law (16) into (14), and rearranging it:

$$\dot{\sigma} = -\kappa \operatorname{sgn}(\sigma) \tag{17}$$

This result is substituted into the derivative of the candidate for the Lyapunov function presented in (13):

$$\dot{\mathcal{V}}(\sigma) = \sigma(-\kappa \operatorname{sgn}(\sigma)) = -\kappa|\sigma| < 0, \sigma \neq 0 \tag{18}$$

where  $\kappa$  is an arbitrary positive constant, thus proving that the selected function is a Lyapunov function where its derivative is negative definite. A saturation function is adopted instead of the sign function to avoid chattering, which is:

$$\operatorname{sat}(\sigma) = \begin{cases} 1 & \text{if } \sigma > \Delta \\ k\sigma & \text{if } |\sigma| \leq \Delta, \quad k = \frac{1}{\Delta} \\ -1 & \text{if } \sigma < -\Delta \end{cases} \tag{19}$$

where a linear boundary layer is established between both positions of the sign function, thus, Fig. 2 illustrates the saturation function utilized in this work.

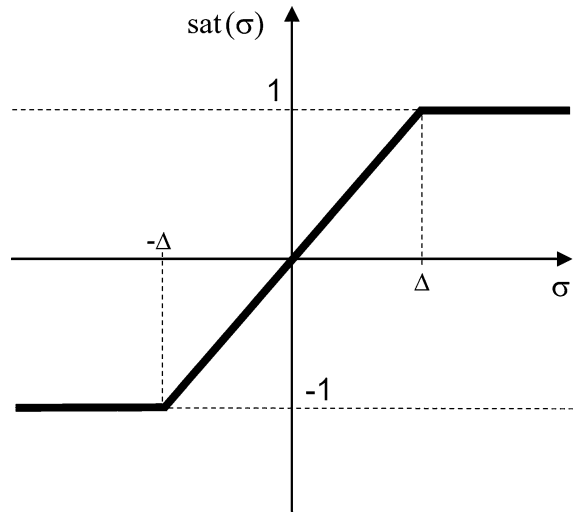


Fig. 2 Saturation function

Thus, the control law can be rewritten with the saturation function:

$$\begin{aligned} [Q]\boldsymbol{\eta} = & \frac{(m_1 - m_2)g \frac{\ell}{2} \sin \theta}{I_{zeq}^O} - \frac{T_{fr}}{I_{zeq}^O} - \ddot{\theta}_d + \\ & + \gamma \dot{e} + \kappa \operatorname{sat}(\sigma) \end{aligned} \tag{20}$$

And it can be rewritten as:

$$[Q]\boldsymbol{\eta} = L \tag{21}$$

where  $L = u_{eq} + u^\pm$ . The sliding mode control law can be separated into two main components, the equivalent ( $u_{eq}$ ) and the switching parts ( $u^\pm$ ). The equivalent component takes place once the system is sliding and the switching component drives the system to the sliding function; where:

$$u_{eq} = \frac{(m_1 - m_2)g \frac{\ell}{2} \sin \theta}{I_{zeq}^O} - \frac{T_{fr}}{I_{zeq}^O} - \ddot{\theta}_d + \gamma \dot{e} \tag{22}$$

and

$$u^\pm = \kappa \operatorname{sat}(\sigma) \tag{23}$$

This sliding mode control law was designed to provide the desired angular acceleration for the reactions wheels. Moreover, we chose to swing up the pendulum using a reaction wheel at a time. To accomplish this task, the control law needs to be rearranged to turn off one of the control modes, i. e., to one of the reaction wheels, an angular acceleration equals to zero is commanded.

Thereby, the sliding mode control law presented in (21) for the 2-RWP can be rewritten such that each control mode can be allocated separately. Thus, the inverse of the  $[Q]$  can be evaluated using a weighted pseudo-inverse as done in [11]:

$$\boldsymbol{\eta} = [W][Q]^T ([Q][W][Q]^T)^{-1} L \quad (24)$$

where for the case of the 2-RWP,  $[W]$  is a  $2 \times 2$  diagonal matrix:

$$[W] = \begin{bmatrix} W_1 & 0 \\ 0 & W_2 \end{bmatrix} \quad (25)$$

where  $W_1$  and  $W_2$  are the weights related to each reaction wheel, respectively. Thus, when it is desired to use only reaction wheel 1:  $W_1 = 1$  and  $W_2 = 0$ , and when using reaction wheel 2:  $W_1 = 0$  and  $W_2 = 1$ .

The swing-up control law can be summarized as:

$$\boldsymbol{\eta}_{sw} = \begin{cases} \boldsymbol{\eta} & \text{if } \text{sgn}(\dot{\theta}) = 1 \\ \boldsymbol{\eta} & \text{if } \text{sgn}(\dot{\theta}) = 0 \\ 0 & \text{if } \text{sgn}(\dot{\theta}) = -1 \text{ and } |\theta| > 20^\circ \\ \boldsymbol{\eta} & \text{if } \text{sgn}(\dot{\theta}) = -1 \text{ and } |\theta| < 20^\circ \end{cases} \quad (26)$$

where  $\boldsymbol{\eta}_{sw}$  is the resulting desired rates for the reaction wheels' angular acceleration, taking into account which reaction wheel is actuating and employing the sliding mode control law designed, and  $\dot{\theta}$  is the pendulum's angular velocity.

This swing-up control strategy is developed to deal with the limitations of the experimental set-up. Moreover, the controller is set to turn-off when the DC motor starts to be unable to provide the necessary torque, i.e., the pendulum's angular position starts to repeat, and the pendulum angular velocity changes its sign. The controller is turned back on when the pendulum reaches another point where the angular position will be repeated, and the angular velocity sign will change again.

In this strategy, the swing-up is always seeking for the sliding function, and it does not switch between controllers. Once the controller is on, the sliding mode control law is responsible for providing adequate angular acceleration for the reaction wheel that is being used. Thus, the motor torque is evaluated, and the voltage is commanded to the DC motor. Additionally, the process of turning off the controller when reaching the saturation of the DC motor uses of the

energy of swinging the pendulum to help to take it to the unstable equilibrium point.

One of the hypotheses made based on experimental observation is that the swing-up control law proposed is only turned off when the pendulum's angular position is in a region different than  $|\theta| < 20^\circ$ , otherwise the sliding mode control actuates.

Thus, the process of swinging up the pendulum will drive the pendulum to the upright position using only a reaction wheel at a time, and the designed sliding mode control law will balance the pendulum in the upright position.

## 4 Results and discussion

This section briefly explains the experimental set-up and reports the two cases studied by this paper, the swing-up and control of an inverted pendulum with two reaction wheels using one of them at a time. The results using reaction wheels 1 and 2 are compared and explained based on the dynamics of the pendulum with two reaction wheels for a better understanding.

The control strategy designed is implemented in an experimental application to verify its performance. The experimental device has a precision potentiometer that measures the pendulum's angular position, a relay module, two PWM control boards, one for each DC motor, and an Arduino Uno prototype platform with a microcontroller. The control law presented in (26) is programmed in the script developed in Arduino.

The real-time controller works as follows: the precision potentiometer evaluates the pendulum's angular position, where the script uses a moving average of five samples to attenuate the noise, and evaluates its derivatives as the difference of consecutive samples divided by the time step. These are the inputs for the control law presented in (26) that evaluates the desired rates for the reaction wheels' angular acceleration. Afterwards, Eqs. (6) and (7) compute the motor torques of the reaction wheels. Here, the reaction wheel mode that is on was already decided, i. e., only one reaction wheel is actuated according to the designer. With these values, Eqs. (8) and (9) calculate the voltages that must be applied to the DC motors. However, the second terms of these equations are neglected because the DC motors do not have encoders; thus, the angular velocities of the

reaction wheels are unknown. These voltages are converted to PWM values from  $-255$  to  $255$  and then commanded to the PWM boards, which are externally fed with  $12\text{ V}$  by power sources. The process is restarted and repeated for the duration of the experiment. Figure 3 illustrates a block diagram to help to understand this process, providing the inputs and outputs of each step of the control strategy. Additional information concerning the experimental device and the low-cost hardware used for the tests can be consulted in [16, 17].

Firstly, Fig. 4 shows the controlled pendulum’s angular position for the two situations investigated in this paper. When actuating using only the reaction wheel 1 (RW1), the pendulum reaches the upright position faster than when using only reaction wheel 2 (RW2). The gains used for all the experiments were  $\kappa = 100$ ,  $\Delta = 1$ , actuating RW1  $\gamma = 2.7$ , and actuating RW2  $\gamma = 2.4$ .

After 10 s, both cases can control the pendulum in the upright position. The swing-up process can be considered slow. However, the hardware used, the self-manufactured pendulum, and its big dimensions have to be taken into account. This series of limitations that the plant imposes to this control problem is responsible for these slower results. Although they emphasize the strength of the control law used, which, despite all the difficulties encountered, manages to swing up and control the pendulum in the upright position with the adaptations made.

Additionally, the difference in the performance between using reaction wheels 1 and 2 can be explained due to the inertia of each one of them. Reaction wheel 2 is smaller and has a lower mass, which implicates in a lower moment of inertia. When considering Eqs. (6) and (7) to calculate the motor torque for the DC motors, it could explain the difference found in the results. The smaller reaction wheel is easier accelerated. However, when analyzing the result depicted in Fig. 4, this does not turn out to be

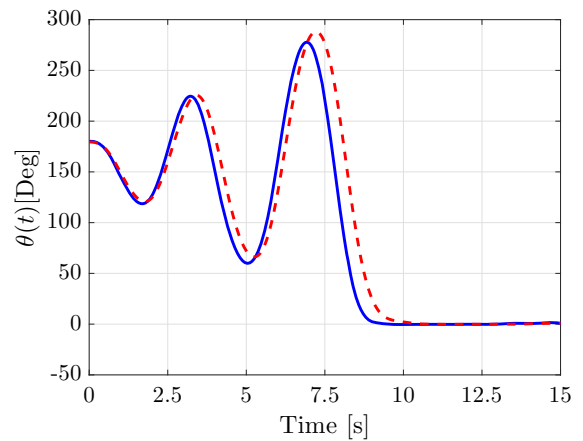


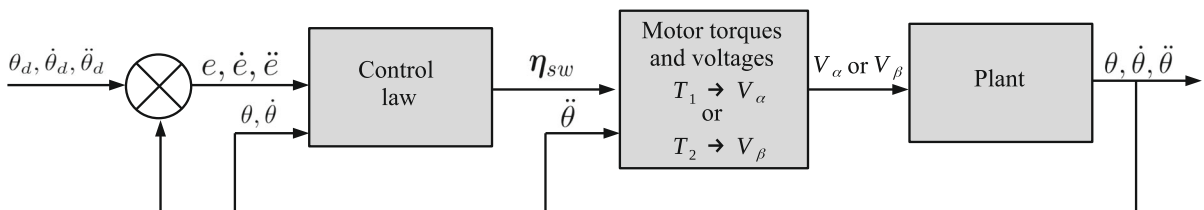
**Fig. 4** Comparison of the experimental pendulum’s angular position to swing up and control the 2-RWP in the upright position ( $\theta = 0^\circ$ ). — actuating RW 1 and - - - actuating RW 2

an advantage, since when actuating reaction wheel 1, the pendulum reaches the upright position faster.

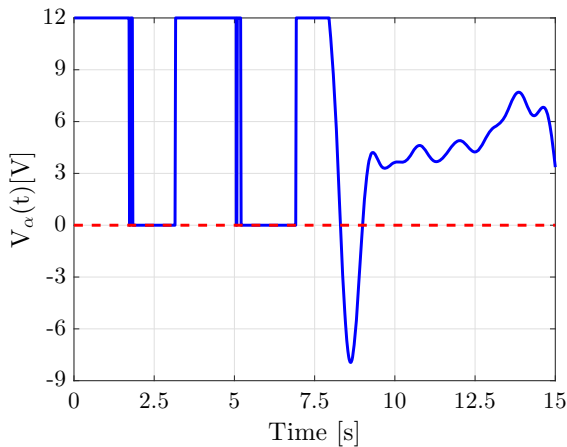
Figure 5 depicts the voltages applied to reaction wheel 1. It is important to highlight that when one of the reaction wheels control modes is off, the voltage should remain at zero, as observed.

Figure 6 presents the voltages applied to reaction wheel 2 and as expected when only reaction wheel 1 is actuated, the voltage of reaction wheel 2 remains at zero.

Since only one reaction wheel is actuated at a time, the voltage applied reaches the DC motor’s saturation limit of  $112\text{ V}$  in the swing-up process. This means that at those instants, the DC motor employs its maximum acceleration capacity. Furthermore, the noise presented in the measurement of the pendulum angular position by the potentiometer causes some imperfections to the controller during the transitions between turning it off and on. This happens because the controller is based on the pendulum angular velocity to be turned off or on. This rate is obtained by deriving the average angular position, which amplifies the



**Fig. 3** Block diagram of the controller operation



**Fig. 5** Comparison of the voltages applied to the DC motor of RW 1 to swing up and control the 2-RWP in the upright position ( $\theta = 0^\circ$ ). — actuating RW 1 and - - - actuating RW 2

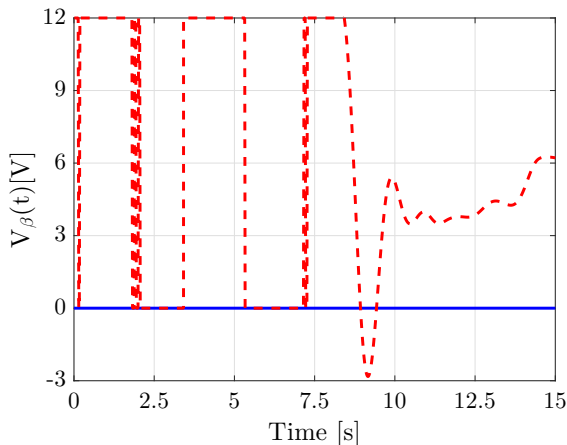


**Fig. 6** Comparison of the voltages applied to the DC motor 2 to swing up and control the 2-RWP in the upright position ( $\theta = 0^\circ$ ). — actuating RW 1 and - - - actuating RW 2

remaining noise. Although this problem can be observed in the transitions, the controller is able to cope with this issue and it does not affect significantly the overall performance.

Moreover, when the pendulum approaches the desired set-point ( $\theta = 0^\circ$ ), the voltages, either using reaction wheel 1 or 2, are not close to the saturation limit and they are almost constant. However, small oscillations can be observed. This happens because we are not fully actuating the system, there are some contributions due to constructions imperfections that were not possible to be modeled once this pendulum

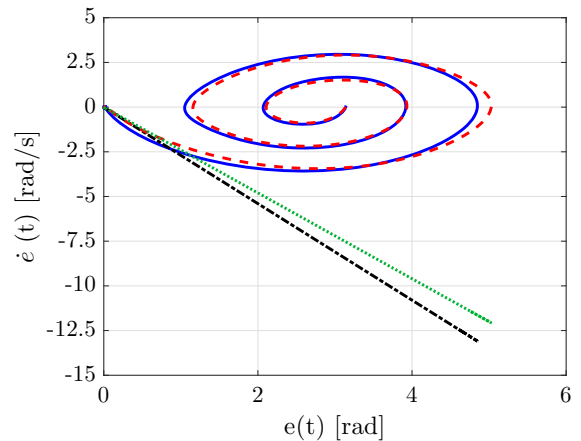


**Fig. 7** Error configuration space with the sliding functions designed. — using RW 1, - - - using RW 2 and -•- the desired sliding function using RW1 and ... the desired sliding function using RW2

was self-manufactured, and there is also the nonlinear behavior of the friction phenomenon.

Figure 7 illustrates the error configuration space in which the sliding function was designed. The swing-up process generates the spirals where we can interpret that one of the control modes was on, and it was not possible to reach the sliding function. And then, the system goes to a farther away position, and it uses the pendulum energy to help in the swing-up process. Thus, a new attempt is made to try to reach the designed sliding function. In the attempt that the pendulum reaches the sliding function, it passes the

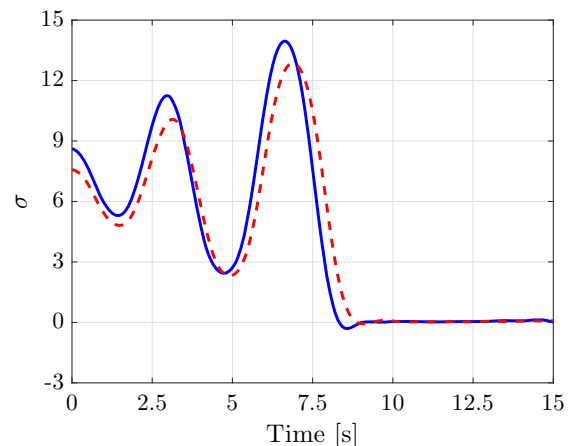


**Fig. 8** Sliding function to swing up and control the 2-RWP in the upright position ( $\theta = 0^\circ$ ) — using RW 1 and - - - using RW 2

function. This also can be seen in Fig. 8, where we show the behavior of the sliding function over time.

Analyzing the behavior of the sliding function over time, we can verify exactly the moment when the control is turned off due to the DC motor's limitations, comparing the time when this occurs to Figs. 5 and 6 in which the voltages applied to the DC motors are presented.

In the controller designed, if the pendulum's angular position is repeated and the pendulum angular velocity changes its signal, the controller is turned off. Thus, the controller will only be turned back on when this happens again, i. e., the pendulum reached another point where its angular velocity was changed. This idea is due to the limitations of the DC motors employed in the plant. The DC motor used for the experimental tests reaches a high angular velocity. This means that low torque is achieved, which is not very interesting for this kind of control strategy. It would be more important than the DC motor provided a higher torque than achieving high angular velocity. From the experimental characterization of the DC motor shown in [16], we can also see that the DC motors used are slow, they have a high time constant  $\tau = 5.88$  s. This is also an issue because even if 12 V is commanded to the DC motors, it takes some time for them to provide the acceleration needed.

Additionally, this paper does not look into an energy approach. We combine a simple swing-up control strategy that deals with the experimental limitations of the plant. We know that the DC motor used does not provide high torques. Therefore, we have chosen to turn off the controller when the torque provided is not enough to reach either the sliding function or the upright position. The disadvantage is that it does not drive the pendulum energy and disk velocity to zero, once the voltages applied to the DC motors for both cases studied are almost constant after the pendulum is controlled in the upright position.

Furthermore, some features make the swing-up and control of the configuration studied in this paper easier than the classical reaction wheel pendulum. In the equation of motion presented in (1), we need to consider to the accompanying term of  $\sin(\theta)$ , that is  $(m_1 - m_2)g\frac{\ell}{2}$ . To model this different configuration, the masses of each DC motors balance themselves. Thus, the term mentioned depends on the reaction wheels' masses difference. However, this

configuration remains an underactuated mechanical system, but this mass difference is smaller than when considering the classical reaction wheel pendulum. Besides, if this new system has both reaction wheels with the same mass, this system is no longer a pendulum, it is a linear system if we do not consider the pendulum friction, and it will not oscillate like a pendulum.

It is essential to state that the strategy presented by this paper was adapted to work within the experimental device when actuating only a reaction wheel at a time. When both reaction wheels are actuated for such configuration, it is not necessary to swing up the pendulum. The real-time implementation of swing-up control strategies in practice is not very simple to be carried out. In this case, an extra challenge is to do so using low-cost hardware costing around USD 150 [16]. The reader can examine the performance of the controller in a video in [1].

## 5 Conclusions

This manuscript presents a novel approach to swing up and control an inverted pendulum with two reaction wheels combining on-off and sliding mode control. The properties achieved using SMC are essential to deal with many of the limitations of the plant, which include the absence of sensors in the DC motors, the low-cost hardware, and the nonlinear behavior of the friction. Additionally, the controller presented is first designed to actuate the system entirely and it is adapted to work using only a reaction wheel. The strategy presents excellent experimental results and is able to swing up the pendulum and control it in the upright position using a single controller.

**Acknowledgements** The authors thank the invitation and recommendation by the 15th International Conference of Dynamical Systems Theory and Applications - DSTA 2019 organizers for the submission of this paper to the special issue *Modeling and analysis of mechanical systems dynamics*. We would like to thank the reviewers and the Editor for their careful revision and useful suggestions.

**Funding** The authors thank the financial support provided by São Paulo Research Foundation (FAPESP) Grant Number 2018/13751-8, and National Council of Technological and Scientific Development (CNPq) Grant Number 306526/2019-0.

## Compliance with ethical standards

**Conflicts of interest** The authors declare that they have no conflict of interest.

## References

1. <https://youtu.be/evk3qk9j9Qs>
2. Adhikary N, Mahanta C (2013) Integral backstepping sliding mode control for underactuated systems: swing-up and stabilization of the cart-pendulum system. *ISA Trans* 52(6):870–880. <https://doi.org/10.1016/j.isatra.2013.07.012>
3. DeCarlo RA, Zak SH, Matthews GP (1988) Variable structure control of nonlinear multivariable systems: a tutorial. *Proc IEEE* 76(3):212–232. <https://doi.org/10.1109/5.4400>
4. Guo ZQ, Xu JX, Lee TH (2014) Design and implementation of a new sliding mode controller on an underactuated wheeled inverted pendulum. *J Franklin Inst* 351(4), 2261–2282 (2014). <https://doi.org/10.1016/j.jfranklin.2013.02.002>. Special issue on 2010–2012 advances in variable structure systems and sliding mode algorithms
5. Gutiérrez-Oribio D, Mercado-Urbe A, Moreno JA, Fridman L (2018) Stabilization of the reaction wheel pendulum via a third order discontinuous integral sliding mode algorithm. In: 2018 15th international workshop on variable structure systems (VSS), pp 132–137. IEEE
6. Hernández VM (2003) A combined sliding mode-generalized pi control scheme for swinging up and balancing the inertia wheel pendulum. *Asian J Control* 5(4):620–625. <https://doi.org/10.1111/j.1934-6093.2003.tb00178.x>
7. Jepsen F, Soborg A, Pedersen AR, Yang Z (2009) Development and control of an inverted pendulum driven by a reaction wheel. In: 2009 international conference on mechatronics and automation, pp 2829–2834. <https://doi.org/10.1109/ICMA.2009.5246460>
8. Neves GP, Angélico BA, Agulhari CM (2019) Robust h2 controller with parametric uncertainties applied to a reaction wheel unicycle. *Int J Control*. <https://doi.org/10.1080/00207179.2018.1562224>
9. Ozana S, Schlegel M (2018) Computation of reference trajectories for inverted pendulum with the use of two-point bvp with free parameters. *IFAC-PapersOnLine* 51(6), 408–413 (2018). In: 15th IFAC conference on programmable devices and embedded systems PDeS. <https://doi.org/10.1016/j.ifacol.2018.07.119>. <http://www.sciencedirect.com/science/article/pii/S2405896318308632>
10. Sanyal AK, Goswami A (2014) Dynamics and balance control of the reaction mass pendulum: a three-dimensional multibody pendulum with variable body inertia. *J Dyn Syst Meas Contr* 136(2):021002
11. Schaub H, Vadali SR, Junkins JL et al (1998) Feedback control law for variable speed control moment gyros. *J Astronaut Sci* 46(3):307–328
12. Shtessel Y, Edwards C, Fridman L, Levant A (2014) Sliding mode control and observation. Springer, Berlin
13. Sowman J, Laila DS, Longo S (2015) Real-time approximate explicit nonlinear model predictive control for the swing-up of a reaction wheel pendulum. In: 2015 54th IEEE conference on decision and control (CDC), pp 4308–4313 (2015). <https://doi.org/10.1109/CDC.2015.7402891>
14. Spong MW, Corke P, Lozano R (2001) Nonlinear control of the reaction wheel pendulum. *Automatica* 37(11):1845–1851. [https://doi.org/10.1016/S0005-1098\(01\)00145-5](https://doi.org/10.1016/S0005-1098(01)00145-5)
15. Srinivas K, Behera L (2008) Swing-up control strategies for a reaction wheel pendulum. *Int J Syst Sci* 39(12):1165–1177. <https://doi.org/10.1080/00207720802095137>
16. Trentin JFS, Cenale TP, da Silva S, de Souza Ribeiro JM (2020) Attitude control of inverted pendulums using reaction wheels: comparison between using one and two actuators. *Proc Inst Mech Eng Part I J Syst Control Eng* 234(3):420–429. <https://doi.org/10.1177/0959651819857643>
17. Trentin JFS, Da Silva S, De Souza Ribeiro JM, Schaub H, Inverted pendulum nonlinear controllers using two reaction wheels (2020) Design and implementation. *IEEE Access* 8:74922–74932. <https://doi.org/10.1109/ACCESS.2020.2988800>

**Publisher's Note** Springer Nature remains neutral with regard to jurisdictional claims in published maps and institutional affiliations.